Electron–phonon coupling in amorphous organic host materials as investigated by photochemical hole burning

J. Friedrich, J. D. Swalen, and D. Haarer

IBM Research Laboratory, San Jose, California 95193
(Received 31 January 1980; accepted 1 April 1980)

The absorption line shapes of photochemical holes of quinizarin in alcohol glasses have been investigated and special attention is given to a detailed analysis of the experimentally observed, intense phonon sidebands at the low energy side of the zero phonon hole. An analytical expression for the shape of these photochemical holes was derived which can be integrated for short burning times. Computer modeling was performed to describe the line shape function in both the short and long burning time limit. These calculations show that there are two contributions to the observed phonon sidebands: One which is due to phonon induced photochemistry and has its maximum on the low energy side of the zero phonon hole and one which is due to zero phonon photochemistry at the laser frequency and has its maximum on the high energy side. It is shown that the various line shape contributions to the photochemical hole have a different burning time behavior. A remarkable feature is that the low energy "pseudo-phonon wing" dominates the direct phonon wing under all experimentally achievable conditions.

I. INTRODUCTION

The electronic spectra of impurity centers in crystalline systems have been investigated extensively and the details of the observed line shapes are well understood; especially the optical spectra of color centers which have been theoretically treated in great detail.[1–3] One feature which makes the interpretation of the observed spectra easy is the appearance of the narrow zero phonon lines (ZPL) whose width is on the order of several wave numbers. These purely electronic transitions are accompanied by well separated phonon sidebands whose widths are on the order of hundreds of wave numbers.[2] The phonon sidebands carry experimental information such as the magnitude and the symmetry of the electron–phonon coupling parameters. Both regimes of strong and weak electron–phonon coupling have been treated theoretically[1] and have led to a good agreement between theory and experiment.

In amorphous glasses the understanding of the optical line shapes is still far from being satisfactory. This is mainly due to two factors: (1) The inhomogeneous broadening, which is about two orders of magnitude larger than in single crystals, obscures details of the spectra, such as zero phonon lines and phonon sidebands. (2) The simple lattice theories, from which one can interpret the optical data with models based on well defined local modes and on the known phonon dispersions, break down.[1]

In this paper we will use photochemical hole burning (PHB) as a tool to remove the inhomogeneous broadening effects of the amorphous glass environment.[4–7] Further we demonstrate that the time dependent change of the observed photochemical hole yields details of electron–phonon coupling strength which are averaged in a straightforward fluorescence line narrowing experiment.[8,9] More specifically, we show that the Debye–Waller factor α which is determined by the electron–phonon coupling strength S varies from site to site over a large range. This is consistent with the notion that many microscopic parameters which characterize glasses vary statistically. S and α are defined as follows:

$$S(T=0)=\sum_k \frac{a_k^2}{2} \tag{1}$$

and

$$\alpha(T=0)=e^{-S}\,, \tag{2}$$

respectively, where a_k is given by

$$a_k=\Delta q_k\left(\frac{\mu_k\omega_k}{\hbar}\right)^{1/2}\,, \tag{3}$$

assuming harmonic potential surfaces and linear electron–phonon coupling. The quantities μ_k and ω_k are the reduced mass and the frequency of the kth mode, respectively. Δq_k is the shift in the equilibrium position which occurs after the excitation process.

In organic crystals one can evaluate the magnitude of the electron–phonon coupling strength of an electronic transition by determining the ratio of the integrated ZPL absorption to its corresponding wing [Eq. (2)]. If *one* specific lattice mode dominates the phonon spectrum, a knowledge of the Debye–Waller factor allows one to determine the frequency of the coupling mode and the related excited state displacement. Examples for system of the above kind are color centers[2] and organic charge-transfer crystals.[11]

In the following we will use the PHB method to shed light on the electron–phonon coupling of the photoreactive center quinizarin (1,4-dihydroxyanthraquinone) in alcohol glass matrices (3:1 EtOH/MeOH).[6,12,13] The experimental observation that the shape of the photochemical hole changes as a function of laser irradiation time will be utilized to extract information about the electron–phonon coupling parameters. Model calculations show that centers of different phonon coupling strengths contribute to the optical line shape at different burning times. Further, a comparison between the experimental hole burning profiles and our numerical calculation demonstrates that the electron–phonon coupling parameters in glasses vary over a wide range.

II. EXPERIMENTAL

Quinizarin was doped into a mixture of ethanol and methanol (3:1) at a concentration of about 10^{-5} mole/

 0021-9606/80/140705-07$01.00

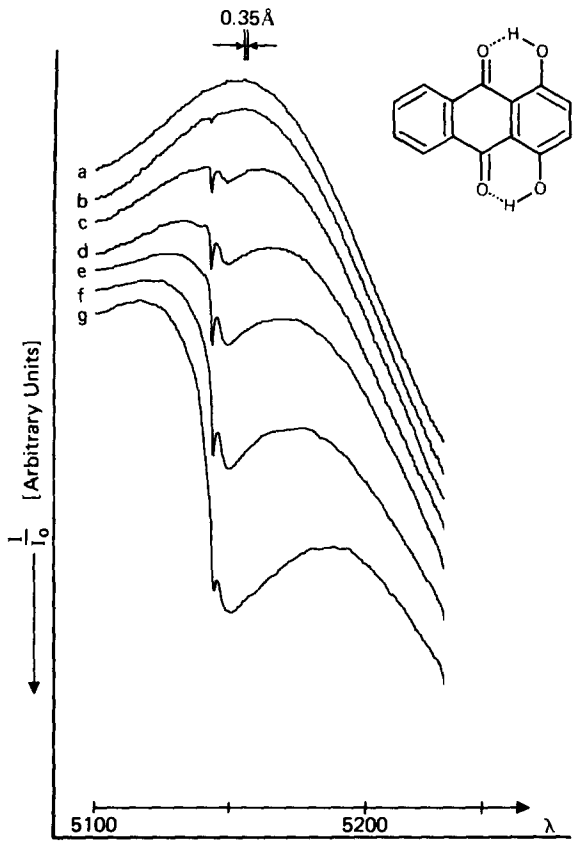

FIG. 1. (a) Experimental inhomogeneous absorption band of the lowest singlet state of quinizarin at 5160 Å. A series of laser photochemical hole burning experiments showing the sharp zero phonon line at the argon ion laser wavelength of 5145 Å and the phonon sideband to longer wave length for times (b) 1 sec, (c) 6 sec, (d) 16 sec, (e) 1 min, (f) 5 min, and (g) 32 min. Each curve has been shifted vertically so as not to overlap the others.

mole. The samples were carefully degassed and sealed in Pyrex cuvettes with an optical path length of 2 mm. Typical optical densities were on the order of 0.1 o.d. The samples were irradiated at 2 °K into the lowest singlet absorption band with either a pulsed dye laser with the bandwidth of 0.1 Å or with the 5145 Å line of a 6 mW argon laser (linewidth $\leq$ 0.04 Å). The photochemical holes were subsequently measured in absorption as a function of irradiation time. The source consisted of a 75 W Xe lamp whose light was spectrally dispersed with a 1 m SPEX monochromator having a slit width of 100 μm and a resolution of 0.35 Å. The signal I/I_0, the current ratio of two red sensitive, cooled photomultipliers, was plotted on a strip chart recorder. The computer calculations were done in APL where the convolution integral (see below for the mathematical details) was evaluated for a series of line shape parameters and Debye-Waller factors. A "best set" was selected by its close agreement by eye to the experimental curves.

III. OPTICAL SPECTRA

The first inhomogeneously broadened singlet absorption band of quinizarin has a half-bandwidth of about 300 cm^{-1} at half-maximum (HWHM) and is centered at 5160 Å. Figure 1, curve (a), shows the broad absorption band before laser irradiation. The subsequent curves (b) through (g) show the band at various stages of the photochemical hole burning. It is seen that the phonon sideband on the low energy side of the zero phonon wing grows steadily and eventually dominates the observed photochemical hole. Note, however, that this broad sideband appears, in contrast to straightforward absorption spectroscopy, at the low energy side of the spectrum.[14,15] We will therefore call this peak the "pseudo-phonon wing" and will show through our calculations that this is a result of photochemical reactions which have been initiated in the real phonon sideband (high energy side) of photochemical centers having their electronic origins at lower energies in the broad inhomogeneous line profile. Our convolution method describes the broad inhomogeneous band as a superposition of zero phonon origins and their associated (real) phonon wings. The laser does photochemical hole burning in the zero phonon bands of several closely related sites overlapping the laser radiation energy and in numerous overlapping phonon wings of sites having their origin at lower energies. The appearance and the shape of a pseudo-phonon wing allow us to estimate the magnitude of the electron-phonon coupling parameters describing the various sites in an amorphous organic matrix such as the EtOH/MeOH glass used for our PHB experiment.

IV. LINE SHAPE MODEL

For a quantitative evaluation of the electron-phonon coupling parameters in amorphous glasses one can perform model calculations which include both the zero phonon contributions and the phonon sideband contributions from an ensemble of photoreactive centers. These calculations allowed us to extract from the experimentally measured hole profiles parameters such as the Debye-Waller factor α. The model calculations also enabled us to verify and check our conclusions from the experiment by computer fitting procedures.

In the following we will make the simplifying assumptions that we can treat the photochemical scheme as a quasi-two-level system and neglect phenomena which are due to ground state depletion. These assumptions seem to be justified if one operates at low laser powers and if none of the intermediate photochemical states are long lived. Both requirements seem to be fulfilled for quinizarin which exhibits PHB at very low laser powers and has no long-lived photochemical intermediates. For the following line shape analysis we adopt the site model, which was used by several authors to explain fluorescence line narrowing.[16-18]

With the above limitations one can describe the photochemical centers by a Gaussian distribution of absorbers with a half-width at half-maximum of Γ_{inh}:

$$\frac{N_0(\nu')}{N} = \sqrt{\frac{\ln 2}{\pi}}\,\frac{1}{\Gamma_{inh}}\exp-\left(\frac{\nu'^2\ln 2}{\Gamma_{inh}^2}\right) . \tag{4}$$

Here $N_0(\nu')$ is the population distribution of molecules at ν' before laser irradiation and N is the total number of absorbing molecules in the ensemble. Absorption

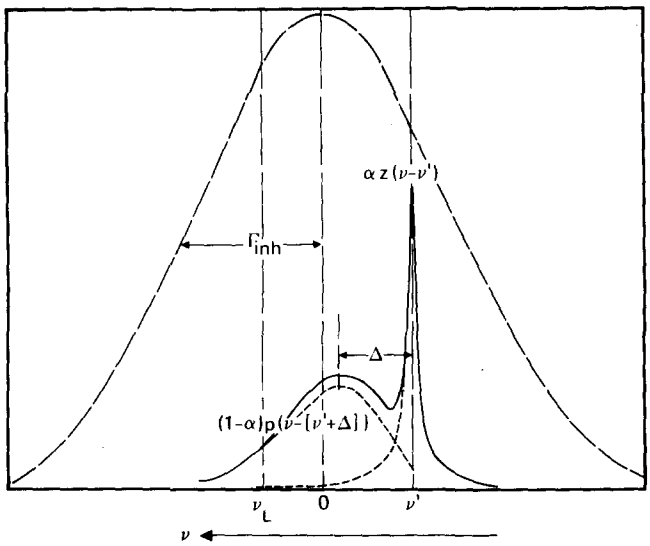

FIG. 2. A schematic showing the inhomogeneous line profile with its half-width at half-maximum Γ_{inh} and the profile of a zero phonon line and its associated phonon sideband for a specific site at frequency ν'. This latter profile has been enlarged compared to the inhomogeneous line to show more detail. The line shape of the zero phonon line is $z(\nu-\nu')$ and that of the phonon sideband, shifted to higher energy by Δ, is $p(\nu-(\nu'+\Delta))$. The Debye-Waller factor is denoted by α and ν_L is the laser frequency.

at ν' is caused by molecules with zero phonon bands or phonon wings overlapping the frequency ν'. The absorption line shape of each individual center is given by a line shape function $g(\nu-\nu')$; it consists of a zero phonon contribution $z(\nu-\nu')$ and of a phonon sideband contribution $p(\nu-(\nu'+\Delta))$. The latter includes a blue shift parameter Δ which gives the displacement of the phonon sideband maximum from the zero phonon origin.

If z and p are normalized, one can express the total absorption line shape of one individual absorber as

$$g(\nu-\nu')=\alpha z(\nu-\nu')+(1-\alpha)p(\nu-(\nu'+\Delta))\,. \tag{5}$$

α is the fraction of the absorption intensity corresponding to the area under the ZPL as defined in Eq. (2) and $(1-\alpha)$ is the fraction under the phonon wing. The inhomogeneous line and a zero phonon band with its associated phonon sideband for one specific site are schematically shown in Fig. 2. The convolution of this asymmetric site pattern over the population distribution leads to a slight skewing of the order of Δ of the inhomogeneous absorption line to higher energy[18] but since $\Delta \ll \Gamma_{inh}$, little effect of this is seen. With an infinitely narrow laser light source at frequency ν_L, one irradiates all molecules according to their absorption strength at ν_L (see Fig. 2). The photochemical reaction will then depend on the molecular absorption cross sections σ, the photochemical quantum yield ϕ, and the photon flux I. With these parameters fixed, one calculates the number of molecules which are left at each frequency ν' after an irradiation time τ:

$$\frac{N_\tau(\nu')}{N}=\sqrt{\frac{\ln 2}{\pi}}\cdot\frac{1}{\Gamma_{inh}}\exp\left(-\frac{\nu'^2\ln 2}{\Gamma_{inh}^2}\right)\cdot C_\tau(\nu_L-\nu')\,,$$

$$\text{where } C_\tau=\exp[-\sigma I\phi\tau g(\nu_L-\nu')]. \tag{6}$$

The related absorption line shape can be obtained from Eq. (6) by a simple convolution technique weighing each center with its molecular line shape function $g(\nu-\nu')$ and integrating over ν':

$$A_\tau(\nu)=\int_{-\infty}^{+\infty}\frac{N_0(\nu')}{N}\cdot C_\tau(\nu_L-\nu')g(\nu-\nu')d\nu'\,. \tag{7}$$

The above Eq. (7) does not make any approximations and will be used for the subsequent computer modeling. First, however, we describe several analytical equations for short burning times τ and for an inhomogeneous linewidth which is large compared to structures in the line shape function $g(\nu-\nu')$. In this limit we treat $N_0(\nu')/N$ as constant and develop the exponential in the last term of Eq. (6) into a power series dropping higher than linear contributions in τ. With these assumptions the following analytical expression, which describes the line shape of the photochemical hole, was derived (short burning time limit):

$$A(\nu)_{t=0}-A(\nu)_{t=\tau}=\sigma\phi I\tau\alpha^2\int_{-\infty}^{+\infty}z(\nu_L-\nu')z(\nu-\nu')d\nu' \tag{8a}$$

$$+\sigma\phi I\tau\alpha(1-\alpha)p\{\nu-(\nu_L+\Delta)\} \tag{8b}$$

$$+\sigma\phi I\tau\alpha(1-\alpha)p\{\nu_L-(\nu+\Delta)\} \tag{8c}$$

$$+\sigma\phi I\tau(1-\alpha)^2\int_{-\infty}^{+\infty}p\{\nu-(\nu'+\Delta)\}\,p\{\nu_L-(\nu'+\Delta)\}d\nu'\,. \tag{8d}$$

Term (8a) represents the zero phonon hole. Its depth grows in a linear fashion with time, and its line shape is given by the following expression, if one assumes a Lorentzian line shape function:

$$\int_{-\infty}^{+\infty}z(\nu_L-\nu')z(\nu-\nu')\,d\nu'=\frac{2\Gamma_h}{\pi}\,\frac{1}{(2\Gamma_z)^2+(\nu-\nu_L)^2} \tag{9}$$

or, in the case of a Gaussian line shape, one gets

$$\int_{-\infty}^{+\infty}z(\nu_L-\nu')z(\nu-\nu')d\nu=\sqrt{\frac{\ln 2}{2\pi}}\cdot\frac{1}{\Gamma_z}\times\exp\left(-\frac{1}{2}\,\frac{(\nu-\nu_L)^2\ln 2}{\Gamma_z^2}\right)\,. \tag{10}$$

The short burning time limit holds with reasonable accuracy ($\lesssim 10\%$) as long as the hole does not exceed about 25% of the total absorption. As pointed out by various authors (see, for example, Ref. 19), the linewidth of the photochemical hole is twice the width Γ_z of the homogeneous line shape function $z(\nu-\nu')$, if z is a Lorentzian. In the case of a Gaussian, the width of the zero phonon hole differs by a factor of $\sqrt{2}$ from the homogeneous line shape. It also follows from Eq. (8a) that the hole width is independent of the burning time in the limit of $t\to 0$.

Terms (8b) and (8c) represent the spectral features of the photochemical hole which are due to the phonon component in the line shape function of the photoactive molecule. In Eq. (8) we have made the assumption that the width of the ZPL is small compared to the width of the phonon side band. The assumption is well fulfilled in our case and allows an integration over ν' in which the ZPL can be approximated by a δ function. Terms (8b) and (8c) have the same intensity and shape and represent the real phonon wing at the high energy side of the ZPL (8b) and the pseudo-phonon wing at the low energy side

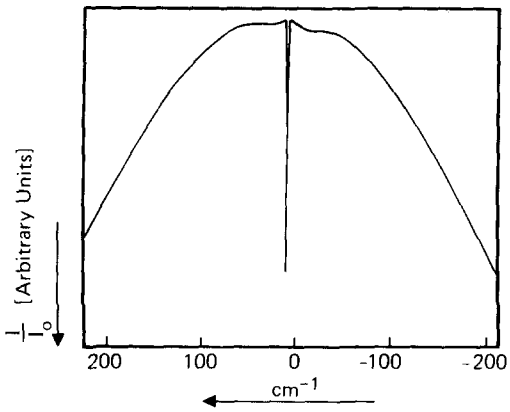

FIG. 3. A calculated zero phonon hole and its associated phonon sideband hole to higher energy and pseudo-phonon sideband hole to lower energy for very short burning times.

of the spectrum (8c). Figure 3 shows a calculation for short burning times. Note that holes from the real phonon wing and the pseudo-phonon wing are approximately equal. We have called (8c) the pseudo-phonon wing because of its unusual spectral position at the low energy side of the ZPL. Both intensity and origin are not related to the zero phonon hole itself and are due to the photochemistry of sites at lower energy which were excited into a phonon level at the laser frequency ν_L. Note that in Eq. (8) the Debye–Waller factor α still gives the correct ratio between the ZPL and the combined ZPL and phonon wing in the limit of weak electron–phonon coupling. Finally, term (8d) is a phonon–phonon term. It can be neglected in the case of small electron–phonon coupling when $(1-\alpha)$ is a small number. This expression (8d) has contributions on both sides of the ZPL.

For long burning times, Eq. (8) breaks down since the ZPL starts to saturate, i.e., all centers having their electronic origin at the laser frequency have been bleached. More and more photochemistry is performed via phonon sideband absorption which leads to a preferential growth of the pseudo-phonon wing (see Fig. 1). In this saturation limit the photochemistry is selectively initiated in the phonon sideband absorption of the photoreactive centers. The observed growth of the pseudo-phonon wing does not, however, allow an accurate determination of the real Debye–Waller without a detailed numerical computer evaluation as will be described below.

V. COMPUTATIONAL

In order to check the validity of the above line shape model, the integration of Eq. (7) was programmed and the absorption $A_\tau(\nu)$ calculated for various sets of parameters. The method consisted of separately calculating a Gaussian zero phonon line and a Gaussian phonon sideband. We restricted, however, the phonon wing from crossing to energies lower than the zero phonon line by constructing the phonon sideband with two half-Gaussian curves of different widths but matched in value at the maximum which was shifted by Δ from the zero phonon line (see Fig. 2). The linewidth Γ'_p of the lower energy half was adjusted so that the phonon wing became sufficiently small at the zero phonon line to make a negligible contribution to $g(\nu-\nu')$ [Eq. (5)]. The area of the zero phonon line was scaled by the Debye–Waller factor α, and the area of the phonon sideband was scaled by $(1-\alpha)$. Two such curves are shown in Fig. 4 for two different Debye–Waller factors. Discrete points of the overall pattern shown in Fig. 4(a) were assigned to the beginning elements of a long vectorial array representing energy, initially 1 cm^{-1} per element but later scaled to better fit the experimental data. It is conceptually convenient to consider a ν' by ν matrix to perform the convolution integral Eq. (7). Every row had the vectorial pattern but was displaced one element from the previous row. At a given row the element at the laser frequency gives $g(\nu_L-\nu')$ which when multiplied by the photochemical coefficient of Eq. (6) gives C_τ. Each row is multiplied by the inhomogeneous line intensity and the photochemical yield at the frequency. Integration [Eq. (7)] was accomplished by summing each column to give the vector $A_\tau(\nu)$.

In order to ensure that the values of the phonon bandwidth, the phonon shift Δ, and the relative ZPL intensity α were close to the experimental values, we performed a series of computations to compare with the experimental hole shape in Fig. 1(d). This comparison is shown in Fig. 5 and the optimal values of the parameters used are listed in Table I.

Figure 6 (upper part) shows the calculated time de-

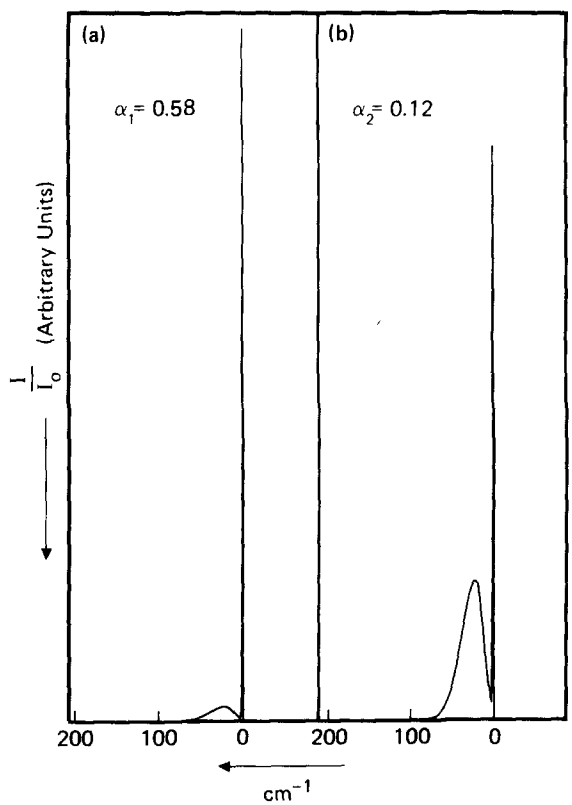

FIG. 4. Two calculated profiles of zero phonon lines and associated phonon sidebands for two different Debye–Waller factors. These profiles are used in the PHB calculated curves shown in Figs. 5 and 6.

TABLE I. Calculational parameters.

Γ_{inh}	300 cm^{-1}
Γ_g	0.4 cm^{-1}
Γ_p	20.0 cm^{-1}
Γ_p'	11.0 cm^{-1}
Δ	21.2 cm^{-1}
α_1	0.58
α_2	0.12

pendence of the photochemical hole. The numerical simulation of the curves show a good agreement with the experimental curves for short-to-intermediate burning times [Figs. 1(a)–(e)].[20] At very short times, Eq. (8) holds with high accuracy and both phonon wings have comparable intensity as is shown in Fig. 3. At longer times curves (e)–(g) in Fig. 6 (lower part) the pseudo-phonon wing tends to dominate the spectrum.

VI. DISCUSSION

In the following we make a more detailed comparison between the measured PHB profiles and the calculated line shapes. The discussion will show the limitations of our numerical calculations and will also shed light on some microscopic parameters such as the electron–phonon coupling of the photoreactive centers in amorphous matrices.

A. Short burning time limit

Even though there is a good quantitative agreement between the early stages of the PHB experiment [Figs. 1(a)–(e)] and the model calculations [Figs. 6(a)–(d)], there are some noticeable differences. In the experiment the ZPL grows steadily from Figs. 1(a)–(e); in the calculation, however, the ZPL reaches its saturation limit[22] at a very early stage [Fig. 6(b)]. From this point on all the additional photochemistry occurs in the pseudo-phonon wing converting photoreactive centers with lower ZPL energies. This latter process of phonon induced photochemistry reaches its saturation at a later stage [Fig. 6(d)] at which the depth of the pseudo-phonon wing approaches the depth of the ZPL. We explain the different saturation behavior of the model calculations and the experiment as follows: In the real experiment one deals with an ensemble of photoreactive centers which have a large variation in electron–phonon coupling parameters, and thus different centers have different ZPL absorption strength. Centers with large α values (small electron–phonon coupling) saturate very early, quite in analogy to the calculations [Figs. 5(a)–(d)] which were performed for comparatively weakly coupled centers. The photochemical centers with large electron–phonon coupling saturate much later and lead to a continued growth of the ZPL at later stages of the PHB experiment.

One phenomenon is quite obvious from both the experiment and the calculation. Only in the very early stage of the calculation is the real phonon wing as intense as the pseudo-phonon wing (see Fig. 3). It is only during this stage that the hole shape and the real line shape function g [Fig. 4(a)] are similar. The measured photochemical holes, however, show a striking asymmetry already during the early stages of PHB. This feature necessarily requires a wide distribution of the involved

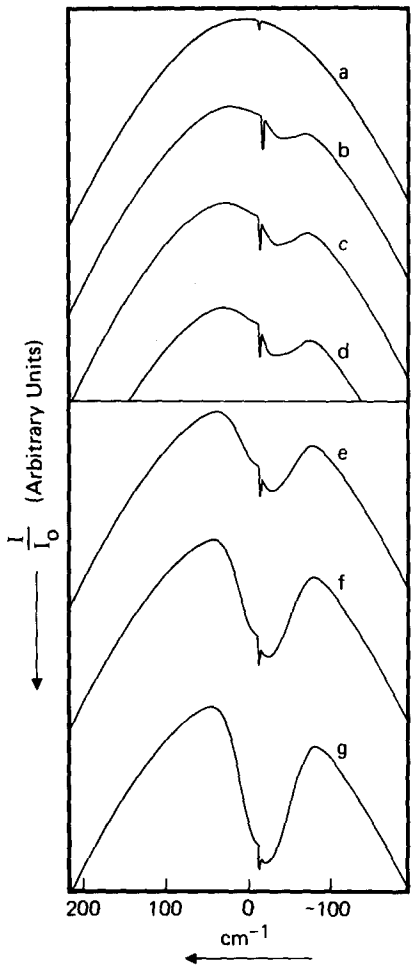

FIG. 6. A series of calculated PHB curves with burning times to approximately match those of Fig. 1. Curves (a) to (d) were calculated with Eq. (7), the parameters in Table I, and the profile in Fig. 4(a). Curves (e) to (g) include the addition of both profiles in Fig. 4.

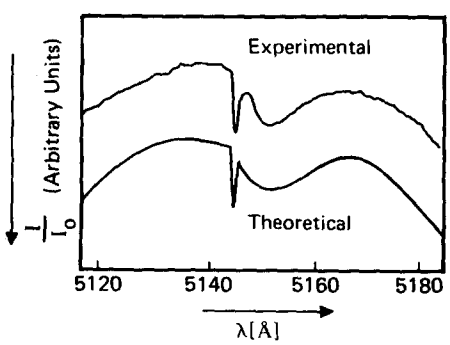

FIG. 5. A comparison of an experimental photochemical hole [from Fig. 1(d)] and a theoretical hole calculated with Eq. (7), the parameters given in Table I, and the profile in Fig. 4(a).

Debye-Waller factors. Given this distribution the pseudo-phonon wing is mainly produced by strongly phonon coupled centers, whereas the direct phonon wing is produced by weakly coupled centers which have a high ZPL absorption at the laser frequency. This interpretation will be used in the subsequent section to describe the long burning time limit.

B. Long burning time limit

In the early burning stage the discrepancy between the experimental and the calculated line shapes was quite subtle, and the only difference was the different saturation behavior of the ZPL. In the intermediate stages and certainly in the late hole burning stages [Figs. 1(f) and (g)], however, the calculation fails to reproduce the measured hole profiles, the main difference being that the experimental curves show appreciable broadening and a rounding off of the hole edges at both sides of the ZPL. This feature plus the above discussed asymmetry is indicative of a larger electron-phonon coupling than had been assumed for the first part of the calculation [see Figs. 4(a) and 6, upper part].

In a complete theory which takes into account the amorphous nature of the host material, one would have to perform calculations in which the electron-phonon coupling strength, given by the parameter α, is treated as a random variable. Similar assumptions of randomly variable parameters had been proposed in various theories of the amorphous state.[10,21] Implementing the assumption of variable α, Eq. (7) has to be averaged over a random distribution of the Debye-Waller factors. The introduction of a random parameter would make our calculation quite complex; therefore, we chose to perform the calculation with two discrete values of α. In the second part of the calculation [Figs. 6(e)-(g)], we selected a line shape function g with an α_2 value, which was a factor of 5 smaller than the one used for the first part of the computer fit. The shape of g is depicted in Fig. 4(b); the numerical hole profiles which result from a continuation of the computer modeling with increased α are depicted in Figs. 6(e)-(g). The main features of this second part of the calculation are similar to those observed in the experiment, namely, a broadening of the photochemical hole at both sides of the ZPL, and a pseudo-phonon hole nearly as deep as the zero phonon hole.

Considering the simplicity of the model and considering the fact that we have taken α not as a random variable but as a superposition of two discrete values, the calculation and the experiment are in good agreement. In the experimental data the very strongly coupled centers (with very small α) seem to show up in the very late burning stage and lead to a pseudo-phonon side band which is deeper than the ZPL [see Figs. 1(f) and (g)]. The calculation which was based on weak and intermediate phonon coupling [using the line shapes function of Figs. 4(a) and (b)] does not reproduce this feature completely. Nevertheless, our present numerical calculations, which are limited to a small number of adjustable parameters, reproduce the observed experimental trends. Finally, we point out that, in principle, this line shape model might be applied to photophysical hole burning experiments as well. However, in this case the "product" is very close in energy.[15] Therefore, it may absorb into its phonon tail at the laser frequency, so that the hole depth is limited by the excited state equilibrium. Then, the system could not be driven in its zero phonon saturation limit.

VII. CONCLUSION

We have presented a line shape model for photochemical holes which includes the phonon structure of the photochemical centers. Treating the electron-phonon coupling as a constant our model shows that the PHB line shape in glasses exhibits, at very early burning stages, a small, symmetric phonon wing at both sides of the ZPL (see Fig. 3).

A comparison between the experimental and the computational line shapes as a function of burning time leads us to the conclusion that the amorphous state is characterized by a large variation in electron-phonon coupling strength. This variation accounts for the observed asymmetry between the real and the pseudo-phonon wing even in the short burning time limit.

At larger burning times the pseudo-phonon wing is the most pronounced feature of the spectral line shape. At this burning stage the ZPL photochemistry reaches saturation and the reaction is dominated by phonon induced photochemistry of strongly coupled centers.

From the presented data we concluded that one has to allow for variations of the Debye-Waller factor of at least a factor of 5 to 10. Even though the calculations have been performed with only two discrete coupling strengths (see Fig. 4) and not with a random distribution of coupling parameters, the agreement between calculation and experiment is quite good.

The above experiments show clearly that site selective experiments, such as PHB, have the potential to shed light on some of the microscopic parameters which describe amorphous solids. It seems to us that PHB has some advantages over methods such as fluorescence line narrowing (FLN), since it introduces a photochemical time domain which, in the above case, enabled us to observe contributions of microscopically different centers at different stages of the photochemical reaction.

ACKNOWLEDGMENT

This work was supported by the ONR.

[1] *Phonons in Perfect Lattices and in Lattices with Point Imperfections*, edited by R. W. H. Stevenson (Plenum, New York, 1966), see Chap. 15 by M. H. L. Pryce.
[2] *Optical Properties of Solids*, edited by J. Nudelman and S. J. Mitra, (Plenum, New York, 1969), see Chap. 21 by R. H. Silsbee.
[3] *Point Defects in Solids*, edited by J. H. Crawford, Jr. and L. M. Sifkin (Plenum, New York, 1972), Vol. 1.
[4] A. A. Gorokhovskii, R.K. Kaarli, and L. A. Rebane, JETP Lett. 20, 216 (1974).
[5] H. de Vries and D. A. Wiersma, Phys. Rev. Lett. **36**, 91 (1976).
[6] F. Graf, H. K. Hong, A. Nazzal, and D. Haarer, Chem.

Phys. Lett. **59**, 217 (1978).
[7]B. M. Kharlamov, R. I. Personov, and L. A. Bykovskaya, Opt. Commun. **12**, 191 (1974).
[8]A. Szabo, Phys. Rev. Lett. **25**, 924 (1970).
[9]A. V. Marchetti, W. C. McColgin, and J. H. Eberly, Phys. Rev. Lett. **35**, 387 (1975).
[10]P. W. Anderson, B. I. Halperin, and C. M. Varma, Philos. Mag. **25**, 1 (1972).
[11]D. Haarer, J. Chem. Phys. **67**, 4076 (1977).
[12]D. M. Burland and D. Haarer, IBM J. Res. Dev. **23**, 534 (1979).
[13]F. Drissler, F. Graf, and D. Haarer, J. Chem. Phys. **72**, 4996 (1980).
[14]A. P. Marchetti, M. Scozzafava, and R. H. Young, Chem. Phys. Lett. **57**, 424 (1977).
[15]J. M. Hayes and G. J. Small, Chem. Phys. **27**, 151 (1978).
[16]I. I. Abram, R. A. Auerbach, R. R. Birge, B. E. Kohler, and J. M. Stevenson, J. Chem. Phys. **63**, 2473 (1975).
[17]W. C. McColgin, A. P. Marchetti, and J. H. Eberly, J. Am. Chem. Soc. **100**, 5622 (1978).
[18]W. C. McColgin, Thesis, University of Rochester, 1975.
[19]S. Voelker, R. M. Macfarlane, A. Z. Genack, H. P. Trommsdorff, and J. H. van der Waals, J. Chem. Phys. **67**, 1759 (1977).
[20]To improve the numerical fit we had to assume that 50%–60% of the absorption strength of the broad inhomogeneous band is due to nonreactive centers, ie.., centers whose local geometry is not favorable for the proposed intermolecular proton transfer.
[21]S. K. Lyo and R. Orbach, Phys. Rev. Lett. (submitted for publication).
[22]We define as saturation the state in which most photoreactive centers with their zero phonon transition at the frequency ν have been transformed into the photoproduct.